

Video Article

In Vitro Assay for Studying the Aggregation of Tau Protein and Drug Screening

Rosa Crespo¹, Wouter Koudstaal¹, Adrian Apetri¹¹Janssen Prevention Center, Janssen Pharmaceutical Companies of Johnson and JohnsonCorrespondence to: Adrian Apetri at aapetri@its.jnj.comURL: <https://www.jove.com/video/58570>DOI: [doi:10.3791/58570](https://doi.org/10.3791/58570)

Keywords: Neuroscience, Issue 141, Tau aggregation, seeding, amyloid, drug screening, Alzheimer's, tauopathies, protein misfolding

Date Published: 11/20/2018

Citation: Crespo, R., Koudstaal, W., Apetri, A. *In Vitro Assay for Studying the Aggregation of Tau Protein and Drug Screening. J. Vis. Exp.* (141), e58570, doi:10.3791/58570 (2018).

Abstract

Aggregation of tau protein and formation of paired helical filaments is a hallmark of Alzheimer's disease and other tauopathies. Compared to other proteins associated with neurodegenerative diseases, the reported *in vitro* aggregation kinetics for tau protein are less consistent presenting a relatively high variability. Here we describe the development of an *in vitro* aggregation assay that mimics the expected steps associated with tau misfolding and aggregation *in vivo*. The assay uses the longest tau isoform (huTau441) which contains both N-terminal acidic inserts as well as four microtubule binding domains (MBD). The *in vitro* aggregation is triggered by addition of heparin and followed continuously by thioflavin T fluorescence in a 96 well microplate format. The tau aggregation assay is highly reproducible between different wells, experimental runs and batches of the protein. The aggregation leads to tau PHF-like morphology which is very efficient in seeding the formation of *de novo* fibrillar structures. In addition to its application in studying the mechanism of tau misfolding and aggregation, the current assay is a robust tool for screening drugs that could interfere with the pathogenesis of tau.

Video Link

The video component of this article can be found at <https://www.jove.com/video/58570/>

Introduction

Alzheimer's disease is a devastating neurodegenerative disorder that is histopathologically defined by the accumulation of extracellular senile plaques of aggregated Amyloid beta¹ and intracellular neurofibrillary tangles containing aggregated hyperphosphorylated tau protein². Physiological tau is monomeric and presented as six unique isoforms containing 0-2 N terminal inserts and 3 or 4 microtubule binding domains^{3,4} arising from alternative splicing and an average of 2-3 phosphorylations. It is believed that hyperphosphorylation, misfolding and self-aggregation into fibrillar structures constitute the key elements in tau pathogenesis, as pathologically assessed in demented individuals^{5,6}.

The aggregated neurofibrillary tau tangles are a hallmark not only for AD but also for other tauopathies, including frontotemporal lobar degeneration (FTLD), Pick's disease, progressive supranuclear palsy (PSP), fronto-temporal dementia (FTD) and primary age-related tauopathy (PART)⁷. From a biochemical point of view, understanding the mechanism of tau misfolding and aggregation could shed light on the pathological processes associated with AD and other tauopathies. In addition to the scientific aspect, robust *in vitro* aggregation assays are valuable tools for screening of drug candidates^{7,8,9,10}. It is believed that the aggregation of tau follows a nucleation dependent polymerization process (NDP)^{11,12,13,14}. The NDP kinetics is sigmoidal and starts with an energetically unfavorable nucleation step followed by a fast energetically downhill aggregation process.

Unlike other amyloidogenic proteins, including the prion protein, amyloid beta and α -synuclein, tau does not spontaneously aggregate under physiological conditions and even extreme pHs or high temperatures are non-conducive for aggregation¹⁵. This is most probably due to the hydrophilic interactions present in the tau aggregation interface. However, tau aggregates efficiently at physiological concentrations when inducers such as heparin¹⁶ or other polyanions^{17,18} are being used.

Previous efforts to set up *in vitro* tau aggregation assays have shed some light onto the details of tau misfolding and aggregation, but they came short of mimicking what is believed to be the *in vivo* tau aggregation kinetics. In most cases, the tau aggregation kinetics was lacking the initial lag phase associated with tau nucleation. This might have been the consequence of using very high tau protein concentrations, presence of aggregates in the starting tau protein preparations and/or use of tau fragments with much higher aggregation propensity than the more physiological full length tau protein^{19,20,21,22,23}. Furthermore, previous studies did not address the reproducibility and robustness aspect of tau aggregation kinetics.

Here, we describe a robust *in vitro* tau aggregation assay which mimics the main characteristics of a nucleation dependent polymerization with an initial lag phase corresponding to the tau nucleation followed by an exponential growth phase. Furthermore, the generated recombinant tau aggregates are fibrillar in nature and have an extremely high seeding potency. The assay is highly reproducible also between tau batches and represents a valuable tool to screen for aggregation inhibitors.

Protocol

1. Reagent Preparation

1. Reaction buffer

1. Prepare reaction buffer: 0.5 mM TCEP in PBS, pH 6.7 by dissolving TCEP dry powder (MW= 286.65 g/mol) in PBS stock solution, pH 7.4.
NOTE: The presence of TCEP is due to bridging aggregation studies using wild type tau protein which contains cysteines. In the current protocol, TCEP is only used to adjust the pH of PBS from 7.4 to 6.7 and plays no role in regulating any redox reactions.
2. Mix thoroughly and filter the solution through a sterile 0.22 μm pore size PES membrane filter.
3. Aliquot and store at $-80\text{ }^{\circ}\text{C}$.
4. Thaw on the bench and stabilize at RT before use.

2. huTau441

1. Remove huTau441 (for protein expression and purification see Apetri *et al.*²⁴) from $-80\text{ }^{\circ}\text{C}$ freezer.
2. Thaw on the bench and equilibrate to room temperature (RT).
3. Spin tube with protein stock for 5 min at 12,000 x g at 20-25 $^{\circ}\text{C}$ to eliminate air bubbles.
4. Measure the concentration of huTau441 by absorption at 280 nm using an extinction coefficient of 0.31 mL $\text{mg}^{-1}\text{cm}^{-1}$

3. Thioflavin T

1. Prepare 500 μM thioflavin T (ThT) stock solution by dissolving 10 mg of ThT dry powder (MW=318.86 g/mol) in 35 mL reaction buffer.
2. Mix thoroughly, vortex 3 times for 20 seconds at maximum speed and filter the solution through a sterile 0.22 μm pore size PES membrane filter.
3. Determine concentration by absorption measurements at 411 nm using an extinction coefficient of 22,000 $\text{M}^{-1}\text{cm}^{-1}$ and adjust ThT concentration to 500 μM . Store at RT protected from light. Prepare fresh every 2 months.

4. Heparin

1. Prepare fresh 55 μM heparin solution by dissolving 1 mg of HMW heparin dry powder (MW = 17-19 kDa) in 1 mL reaction buffer at RT.
2. Shake vigorously and vortex 2 times for 5 seconds.
3. Filter solution through a sterile 0.20 μm pore size PES membrane filter (syringe).

2. Continuous Mode ThT Aggregation Assay on a Multi-Mode Microplate Reader

NOTE: ThT dye is added to the reaction to monitor huTau441 aggregation kinetics in a continuous mode (automatic measurements). Although the reaction can be followed by a regular fluorometer using a conventional cuvette, the manual nature of the operation limits the frequency of measurements and compromises the accuracy of the recorded kinetic curves. For this reason, an automatic multi-mode microplate reader is used.

1. Instrument set up

1. Turn on the computer and the multi-mode microplate reader. Let the equipment stabilize for 10 minutes.
2. Start the software and prepare a protocol.
 1. Select the protocol type: standard protocol (Data reduction is performed independently for each plate).
 2. Set the temperature at 37 $^{\circ}\text{C}$ and select preheat before continuing the protocol.
 3. Set the kinetic run: Run Time 50 h / Measurement interval: 15 min.
 4. Set orbital shaking at 425 cpm (3 mm) in continuous mode.
 5. Select the read method: Fluorescence intensity - Endpoint/Kinetic - Monochromators Wavelengths: Excitation 440 nm (20 nm bandwidth) / Emission 485 nm (20 nm bandwidth) - Optics position: Top - Normal read speed - Read height: 4.50 mm
 6. Start the run using the created protocol. Name the experiment, select the destination of the newly created file and allow the instrument to pre-equilibrate to desired temperature.

2. Spontaneous huTau441 conversion

1. Prepare the reaction sample in a 1.5 mL tube. Use 200 μL mix per reaction and at least 4 replicates (reaction volume for 4 replicates = 800 μL).
2. Prepare 800 μL reaction sample (in case of 4 replicates) containing 15 μM huTau441, 8 μM heparin and 50 μM ThT. Start by mixing the protein with the reaction buffer, add heparin and ThT and mix well by pipetting up and down 5 times. Respect the indicated order for reagent addition.
3. Spin samples at 12,000 x g and 25 $^{\circ}\text{C}$ for 5 min to eliminate air bubbles.
4. Dispense 200 μL of reaction sample per well in 96-well microplates (96-well black solid microplate, well-volume 360 μL , flat bottom). Avoid formation of air bubbles.
5. Seal microplate to avoid evaporation.
6. Place microplate in multi-mode microplate reader and start measurements.
7. After completion of experiment, remove plate from equipment and export data to a data processing software.

3. Quality check of the conversion, seed collection and storage.

1. Remove the sealer from the plate and pool the different replicates in 1.5 mL tubes. Mix well the aggregated sample in the wells by pipetting up and down 2 times before collecting it. Aggregates tend to deposit on the bottom of the well.

2. Mix thoroughly in the 1.5 mL tube by pipetting up and down 5 times and dispense 10-20 μL on a mica surface for analyzing the aggregates by AFM (for further details see Apetri *et al.*²⁴).
 3. Harvest the aggregates by spinning the 1.5 mL tube at 20,000 x g and 4 °C for 1 hour. Aggregates form a pellet.
 4. Separate and analyze supernatant by S-MALS to confirm the absence of monomeric tau in the sample indicating a successful conversion into aggregates (for further details see Apetri *et al.*²⁴).
 5. Label the 1.5 mL tube containing the remaining aggregates (pellet) indicating initial huTau441 protein concentration and sample volume. Snap freeze the aggregates and store at -80 °C.
4. **Seeded reaction**
1. Remove huTau441 aggregates from -80 °C freezer. Add the volume of reaction buffer indicated on the label (initial sample volume) and let the tube stabilize to RT. Resuspend the aggregates by pipetting up and down 5 to 8 times.
 2. Sonicate the aggregated sample. For a 200 μL sample (15 μM huTau441), sonicate on ice using a 1/8" microtip (from 100 μL up to 10 mL) for a total period of 15 s using pulses of 1 s and pauses of 2 s at 30% amplitude (sonicator 250 Watts). Re-equilibrate sample to RT.
NOTE: The employed sonication conditions lead to a homogeneous population of tau fibrils with lengths of 20-50 nm²⁴.
 3. Prepare the reaction sample in 1.5 mL tubes. Use 200 μL mix per reaction and at least 4 replicates (reaction volume for 4 replicates = 800 μL).
 4. Prepare 800 μL reaction sample containing 15 μM huTau441, 8 μM heparin and 50 μM ThT. Start by mixing the protein with the reaction buffer, add heparin and ThT and mix well by pipetting up and down 5 times. Respect the indicated order for reagent addition.
 5. Spin samples at 12,000 x g and 25 °C for 5 min to eliminate air bubbles.
 6. Dispense 200 μL of reaction sample per well in 96-well (96-well black solid microplate, well-volume 360 μL , flat bottom). Avoid formation of air bubbles.
 7. Homogenize thoroughly the preformed fibril sample by repetitive up and down pipetting (5 times) and add to each well the amount corresponding to the desired percentage of seeds. For a 200 μL well total volume, 2 μL of preformed seed addition is a 1% (v/v). Mix by pipetting up and down 3 times when adding to the well and avoid formation of air bubbles.
 8. Seal microplate to avoid evaporation.
 9. Place microplate in multi-mode microplate reader and start measurements.
 10. Remove plate from equipment and export data to a spreadsheet.

Representative Results

Recombinant huTau441 containing the C291A and C322A mutations and N-terminal His and C-terminal C-tags was expressed and purified as previously described²⁴. The huTau441 batches are highly pure as visualized on SDS-PAGE and virtually 100% monomeric as assessed by S-MALS (**Figure 1**). The aggregation of 15 μM huTau441 was induced by the addition of 8 μM HMW heparin and the reaction was followed continuously by ThT fluorescence using a multimode microplate reader. The excitation wavelength was 440 nm (bandwidth 20 nm) whereas emission was measured at 485 nm (bandwidth 20 nm). The assay is highly reproducible, with results from 10 individual wells being virtually indistinguishable (**Figure 2A**). The morphologies of the ThT positive huTau441 aggregates were assessed after 50 h by AFM. Aggregated huTau441 is a homogeneous mixture of fibrillar structures of different lengths similar to reported *ex vivo* morphologies (**Figure 2B**). Furthermore, the final reaction mixture does not contain monomer, suggesting a full conversion into aggregates as shown by S-MALS measurements (**Figure 2C**). The kinetics of huTau441 aggregation in independent experimental runs are very similar as emphasized by similar sigmoidal curves and indistinguishable lag and growth phases (**Figure 3**). The high level of reproducibility is maintained when different batches of protein are used (**Figure 4**). Furthermore, preformed huTau441 aggregates are very efficient in recruiting tau monomer and inducing formation of *de novo* tau aggregates. Amounts as low as 0.0025% (v/v) of preformed tau aggregates are capable to bypass nucleation and trigger generation of *de novo* fibrils (**Figure 5**).

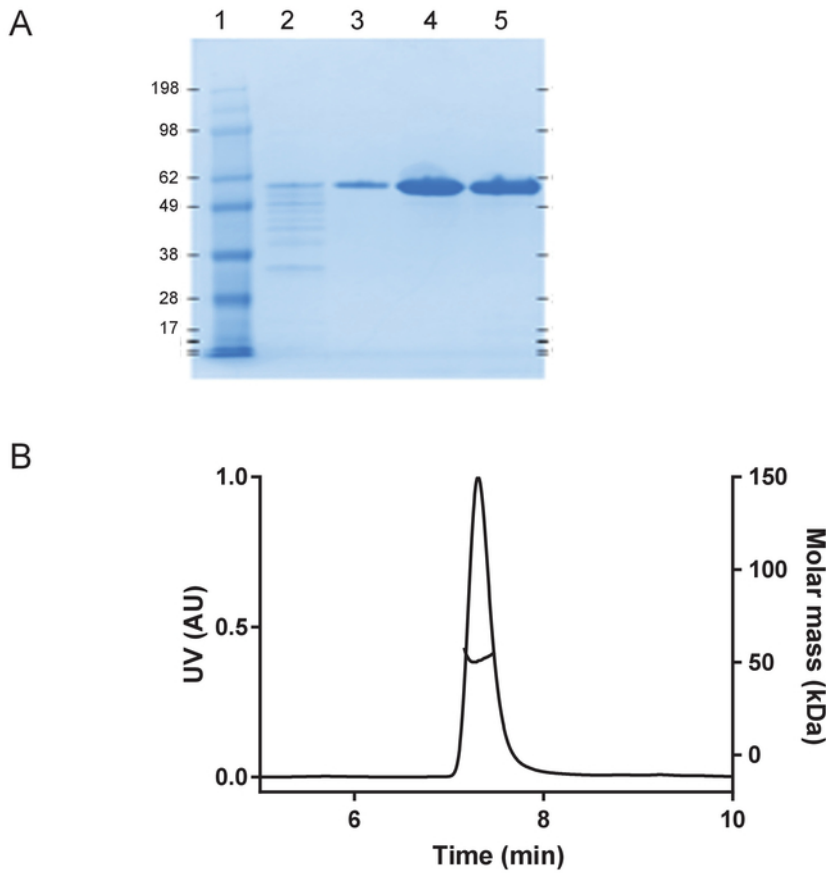


Figure 1: Recombinant huTau441 is monomeric and highly pure. A) Purity assessment under denaturing conditions on a 4-12% SDS-PAGE gel including molecular weight standard protein ladder (in kDa) (Lane 1); flow through from the final C-tag affinity purification step (Lane 2); column wash fraction (Lane 3), eluted huTau441 protein peak, before (Lane 4) and after buffer exchange (Lane 5), respectively). B) S-MALS analysis of the huTau441. Protein shows to be > 99.9% monomeric with a molar mass of 51 kDa and does not contain aggregates or fragments. [Please click here to view a larger version of this figure.](#)

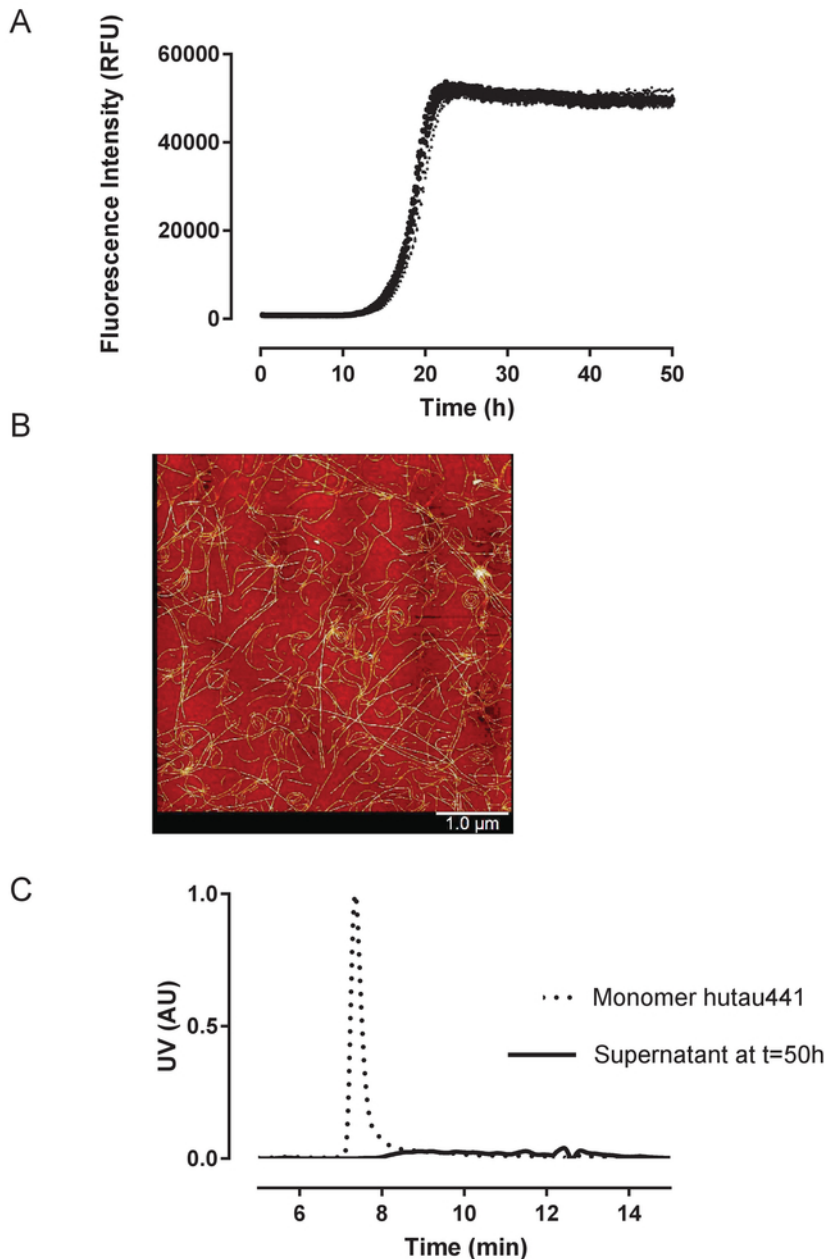


Figure 2: Aggregation of recombinant huTau441 is highly reproducible and leads quantitatively to fibrillar structures. A) Kinetics of heparin induced huTau441 aggregation monitored continuously in 96 well microplate format by ThT fluorescence. Concentrations of huTau441 and heparin are 15 μM and 8 μM , respectively. The 10 individual curves correspond to the conversion of the same protein batch in ten wells of the same microplate and are characterized by an average (with SD) lag phase of 14.2 ± 0.38 h and t_{50} of 18.8 ± 0.40 h. Kinetic data was fitted with a 5-parameter logistic curve with a linear decline in the upper asymptote. Lag phase and t_{50} were calculated by interpolation between predicted values by linear regression. Lag phase is calculated based on the 3% increase of ThT fluorescence signal. Curve fitting and summary statistics are obtained using IBM SPSS statistics version 20.0.0.2. B). Tau aggregates show PHF-like morphologies as indicated by AFM imaging at 50 h; C). S-MALS analysis of monomeric huTau441 ($t = 0$ h) and the supernatant of the reaction mixture at the completion of the reaction ($t = 50$ h). At the 50 h time point the reaction mixture was centrifuged for 1h at 20,000 X g and 4 $^{\circ}\text{C}$ and the resulted supernatant injected on S-MALS. The disappearance of the monomer peak confirms the complete aggregation of tau. [Please click here to view a larger version of this figure.](#)

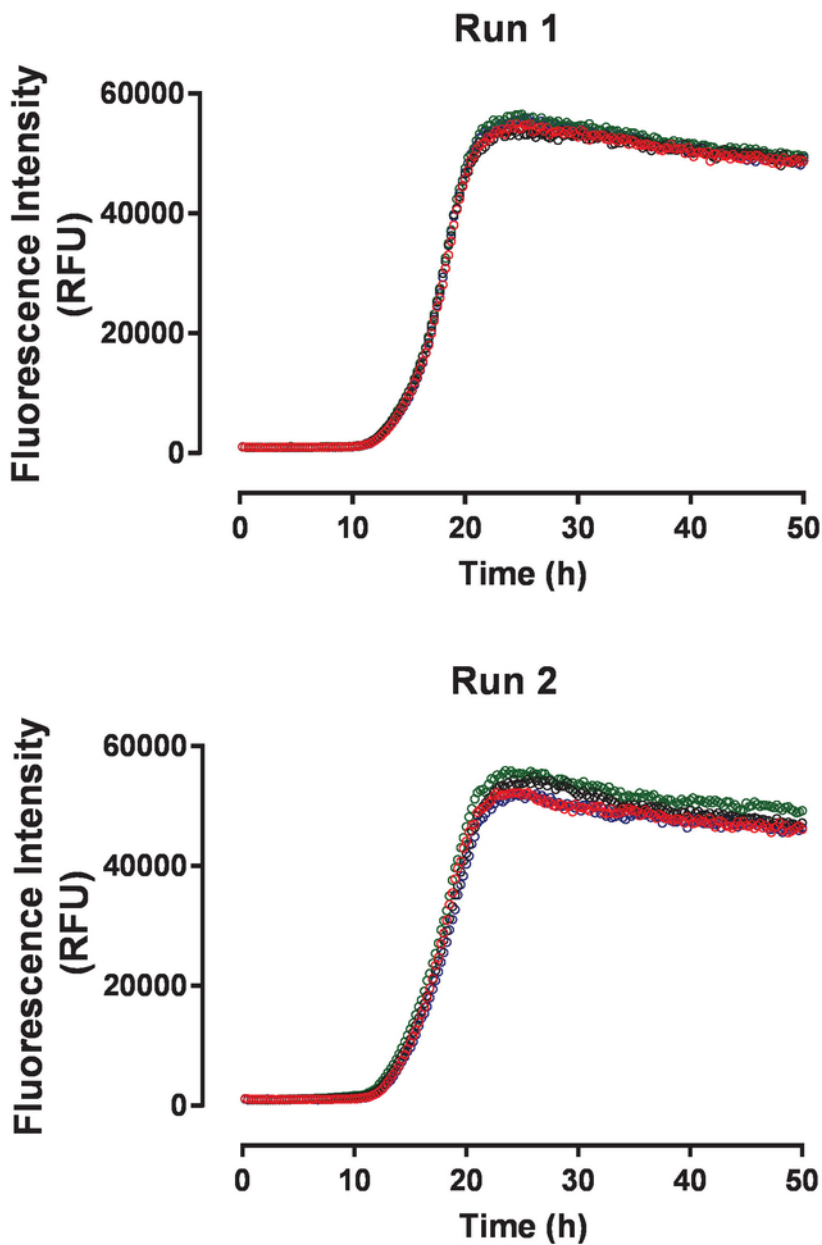


Figure 3: The tau aggregation assay shows high reproducibility between independent experimental runs. The two panels display four individual kinetics traces for spontaneous huTau441 aggregation collected in two independent experiments using the same batch of huTau441 protein. Concentrations of huTau441 and heparin are 15 μ M and 8 μ M, respectively. Kinetics are characterized by an average (with SD) lag phase of 12.2 ± 0.18 h and t_{50} of 17.8 ± 0.8 h (Run 1) and 11.6 ± 0.52 h and t_{50} of 17.8 ± 0.23 h (Run 2), respectively. Kinetic data was fitted with a 5-parameter logistic curve with a linear decline in the upper asymptote. T_{50} were calculated by interpolation between predicted values by linear regression. Lag phase is calculated based on the 3% increase of ThT fluorescence signal. [Please click here to view a larger version of this figure.](#)

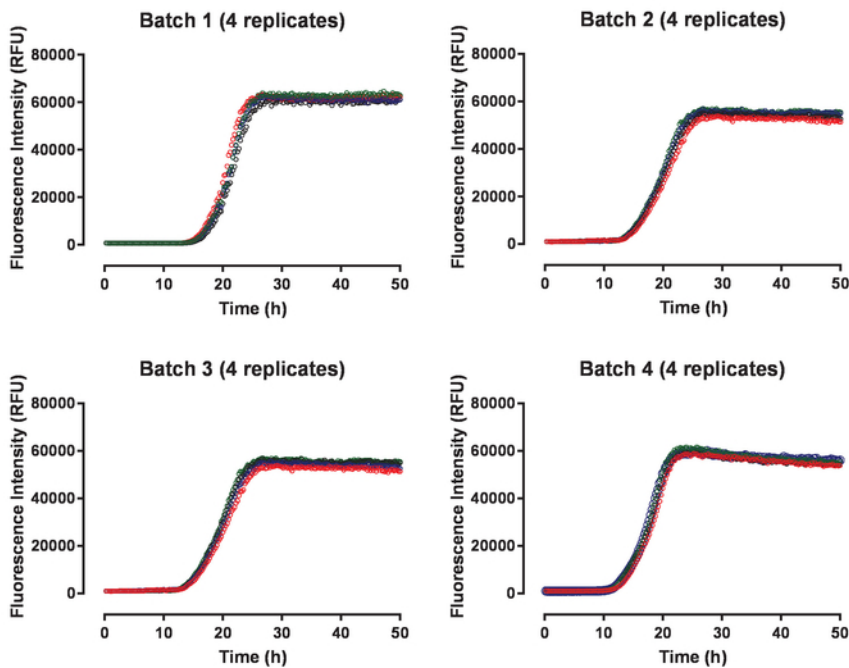


Figure 4: The tau aggregation assay shows high reproducibility between different batches of huTau441 protein. Each panel shows four replicates corresponding to a specific huTau441 batch. The aggregation of each batch was followed in independent experiments. Concentrations of huTau441 and heparin are 15 μ M and 8 μ M, respectively. Aggregation kinetics corresponding to the four individual tau batches are characterized by an average (with SD) lag phase of 15.3 ± 0.38 h and t_{50} of 21.1 ± 0.46 h (Batch 1); lag phase of 12.5 ± 0.07 h and t_{50} of 19.8 ± 0.34 h (Batch 2); lag phase of 15.1 ± 0.34 h and t_{50} of 21.9 ± 0.86 h (Batch 3) and lag phase of 11.5 ± 0.29 h and t_{50} of 17.8 ± 0.29 h (Batch 4), respectively. Kinetic data was fitted with a 5-parameter logistic curve with a linear decline in the upper asymptote. Lag phase and t_{50} were calculated by interpolation between predicted values by linear regression. Lag phase is calculated based on the 3% increase of ThT fluorescence signal. [Please click here to view a larger version of this figure.](#)

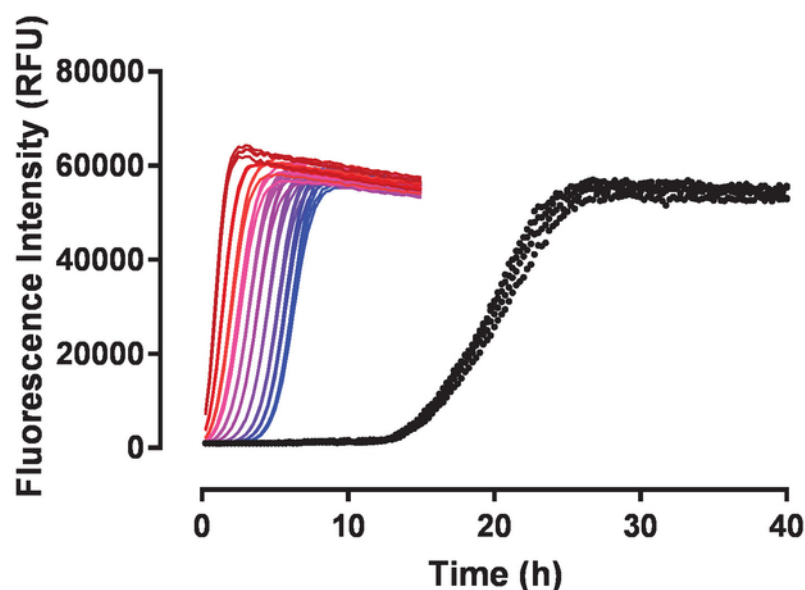


Figure 5: Preformed hutau441 aggregates have high seeding activity. To initiate seeding, sonicated tau aggregates were added to monomer hutau441. From red to blue, each color of the different kinetic curves represents the different amount of added seeds: 1.25%, 0.63%, 0.31%, 0.16%, 0.08%, 0.04%, 0.02%, 0.01%, 0.005% and 0.0025% (v/v), respectively. Spontaneous conversion of hutau441 is represented in black. All conditions were tested in quadruplicate. The four kinetic replicates associated with a certain concentration of seeds are highly reproducible and in most cases indistinguishable. Concentrations of hutau441 and heparin are 15 μ M and 8 μ M, respectively. The addition of small amounts of pre-formed sonicated fibrillar structures eliminates the initial lag phase observed in the spontaneous conversion and the effect is proportional with the amount of seeds. From red to blue, the difference in t_{50} observed (t_{50} spont.conv- t_{50} seeding) is 18.9, 18.40, 17.8, 17.3, 16.6, 16.1, 15.4, 14.7, 14.2 and 13.7 hours, respectively. Spontaneous conversion of hutau441 is characterized by an average t_{50} (with SD) of 19.85 ± 0.54 h. Kinetic data was fitted with a 5-parameter logistic curve with a linear decline in the upper asymptote. t_{50} were calculated by interpolation between predicted values by linear regression. [Please click here to view a larger version of this figure.](#)

Discussion

Despite numerous efforts, the tau aggregation kinetics reported in the literature to date lack the desired level of reproducibility and/or some of the features of a nucleation dependent polymerization^{19,20,21,22,23,25}. This is often emphasized by the lack of a lag phase, inefficient seeding and non-fibrillar nature of tau aggregates. The reason for these shortcomings can vary and includes sub-optimal tau protein quality (fragmentation, presence of aggregates, low purity, etc.), choice of protein and inducing reagents and or experimental conditions. Another complicating factor are the two cysteine residues located around the tau aggregation interface that can form intra- or inter- molecular disulfide bridges depending on the redox environment and affect the efficiency of tau aggregation. In most approaches reducing reagents such as DTT or TCEP have been used to maintain the cysteine residues in reduced forms and thus increase levels of reproducibility²⁵. Furthermore, the extinction coefficient of tau is very low which leads to difficulties in accurate measurements of protein concentration.

We focused especially on a few parameters and quality attributes that we considered crucial for a robust, reproducible and representative aggregation profile for tau protein: eliminating the possibility of intra- and inter- molecular disulfide formation, generating a highly pure tau monomer and improving the accuracy of concentration determination. All these reagent related questions are potential attention points that we considered critical for optimal assay development. To address these issues, full length huTau441 was expressed with two mutations, C291A and C322A, and with N- and C- terminal tags. Mutation of the cysteine residues has minimal impact on the tau protein while eliminating the otherwise very difficult to control disulfide bridging. Expressing the protein with relatively short N- and C- terminal tags allowed us to pursue a two-step affinity purification protocol which led to very high purity, integrity and monomer content. Furthermore, we introduced a F8W mutation that increased the extinction coefficient of the protein and allowed much more accurate concentration measurements²⁴.

In addition to using high-quality protein reagents, other assay parameters were also optimized. The optimal tau : heparin ratio was identified to be around 0.5 (M/M) which is in line with previously published studies²⁶. Furthermore, mechanical and optical instrumental settings are crucial to ensure reproducibility and the optimal parameters might differ to some extent depending on the manufacturer.

The aggregation of tau described in this assay shows characteristics that are associated with tau pathogenesis in AD and related tauopathies. The process starts with an initial lag phase corresponding to the formation of high energy nuclei and is followed by a rapid growth phase that corresponds to fibril growth. The lag time is sufficiently long to open a broad window to study in detail the seeding process covering a broad range of seed concentrations (Figure 5) while still not too long so protein degradation and/or non-specific aggregation are avoided (Figure 2). These secondary events could especially happen when an intrinsically disordered protein such as huTau441 is exposed for long periods of time to physiological conditions. The obtained tau aggregates display the morphology of PHFs isolated from brains of AD patients and are very efficient in recruiting monomeric tau and converting it to *de novo* generated aggregates, a process referred to as seeding. The assay is highly reproducible, the kinetic curves being virtually indistinguishable between wells, experimental runs and protein batches. Although the current

assay focuses only on the longest tau isoform, huTau441, the application can be adapted to study the conversion of other forms of tau (Ameijde *et al.*, *Acta Neuropathologica Communications*, in press) Furthermore, it enables mechanistic studies focused on the interplay of tau isoforms and possibly shed light on the differences between tau pathogenesis in AD where both 3R and 4R isoforms are present in PHFs and PICK's disease or Frontotemporal dementia where tau pathology contains mainly 3R and 4R tau isoforms, respectively²⁷.

The very high reproducibility of the assay should allow readers to implement it with relative ease in their specific lab settings. The assay mimics what is believed to be the *in vivo* misfolding and aggregation of tau, enabling mechanistic studies that will shed light on tau pathogenesis and it constitutes a valuable tool for screening drug candidates and evaluate their interference with the different steps of the pathogenesis process.

Disclosures

The authors have nothing to disclose.

Acknowledgements

The authors would like to thank Hector Quirante for the expression and purification of huTau441, Hanna Inganäs and Margot van Winsen for excellent technical support and Martin Koldijk for data analysis.

References

1. Querfurth, H. W., & LaFerla, F. M. Alzheimer's disease. *The New England Journal of Medicine*. **362** (4), 329-344, (2010).
2. Lee, V. M., Goedert, M., & Trojanowski, J. Q. Neurodegenerative tauopathies. *Annual Review of Neuroscience*. **24** 1121-1159, (2001).
3. Goedert, M., Wischik, C. M., Crowther, R. A., Walker, J. E., & Klug, A. Cloning and sequencing of the cDNA encoding a core protein of the paired helical filament of Alzheimer disease: identification as the microtubule-associated protein tau. *Proceedings of the National Academy of Sciences of the United States of America*. **85** (11), 4051-4055, (1988).
4. Himmler, A., Drechsel, D., Kirschner, M. W., & Martin, D. W., Jr. Tau consists of a set of proteins with repeated C-terminal microtubule-binding domains and variable N-terminal domains. *Molecular and Cellular Biology*. **9** (4), 1381-1388, (1989).
5. Mandelkow, E., von Bergen, M., Biernat, J., & Mandelkow, E. M. Structural principles of tau and the paired helical filaments of Alzheimer's disease. *Brain Pathology*. **17** (1), 83-90, (2007).
6. Lee, V. M., Balin, B. J., Otvos, L., Jr., & Trojanowski, J. Q. A68: a major subunit of paired helical filaments and derivatized forms of normal Tau. *Science*. **251** (4994), 675-678, (1991).
7. Wischik, C. M., Harrington, C. R., & Storey, J. M. Tau-aggregation inhibitor therapy for Alzheimer's disease. *Biochemical Pharmacology*. **88** (4), 529-539, (2014).
8. Pickhardt, M. *et al.* Identification of Small Molecule Inhibitors of Tau Aggregation by Targeting Monomeric Tau As a Potential Therapeutic Approach for Tauopathies. *Current Alzheimer Research*. **12** (9), 814-828, (2015).
9. Paranjape, S. R. *et al.* Azaphilones inhibit tau aggregation and dissolve tau aggregates *in vitro*. *ACS Chemical Neuroscience*. **6** (5), 751-760, (2015).
10. Seidler, P. M. *et al.* Structure-based inhibitors of tau aggregation. *Nature Chemistry*. **10** (2), 170-176, (2018).
11. Apetri, A. C., Vanik, D. L., & Surewicz, W. K. Polymorphism at residue 129 modulates the conformational conversion of the D178N variant of human prion protein 90-231. *Biochemistry*. **44** (48), 15880-15888, (2005).
12. Crespo, R., Rocha, F. A., Damas, A. M., & Martins, P. M. A generic crystallization-like model that describes the kinetics of amyloid fibril formation. *Journal of Biological Chemistry*. **287** (36), 30585-30594, (2012).
13. Holmes, B. B. *et al.* Proteopathic tau seeding predicts tauopathy *in vivo*. *Proceedings of the National Academy of Sciences, USA*. **111** (41), E4376-4385, (2014).
14. Surewicz, W. K., Jones, E. M., & Apetri, A. C. The emerging principles of mammalian prion propagation and transmissibility barriers: Insight from studies *in vitro*. *Accounts of Chemical Research*. **39** (9), 654-662, (2006).
15. Jeganathan, S., von Bergen, M., Mandelkow, E. M., & Mandelkow, E. The natively unfolded character of tau and its aggregation to Alzheimer-like paired helical filaments. *Biochemistry*. **47** (40), 10526-10539, (2008).
16. Goedert, M. *et al.* Assembly of microtubule-associated protein tau into Alzheimer-like filaments induced by sulphated glycosaminoglycans. *Nature*. **383** (6600), 550-553, (1996).
17. Kampers, T., Friedhoff, P., Biernat, J., Mandelkow, E. M., & Mandelkow, E. RNA stimulates aggregation of microtubule-associated protein tau into Alzheimer-like paired helical filaments. *FEBS Letters*. **399** (3), 344-349, (1996).
18. Wilson, D. M., & Binder, L. I. Free fatty acids stimulate the polymerization of tau and amyloid beta peptides. In vitro evidence for a common effector of pathogenesis in Alzheimer's disease. *American Journal of Pathology*. **150** (6), 2181-2195, (1997).
19. Barghorn, S., & Mandelkow, E. Toward a unified scheme for the aggregation of tau into Alzheimer paired helical filaments. *Biochemistry*. **41** (50), 14885-14896, (2002).
20. Friedhoff, P., Schneider, A., Mandelkow, E. M., & Mandelkow, E. Rapid assembly of Alzheimer-like paired helical filaments from microtubule-associated protein tau monitored by fluorescence in solution. *Biochemistry*. **37** (28), 10223-10230, (1998).
21. Morozova, O. A., March, Z. M., Robinson, A. S., & Colby, D. W. Conformational features of tau fibrils from Alzheimer's disease brain are faithfully propagated by unmodified recombinant protein. *Biochemistry*. **52** (40), 6960-6967, (2013).
22. Ramachandran, G., & Udgaonkar, J. B. Mechanistic studies unravel the complexity inherent in tau aggregation leading to Alzheimer's disease and the tauopathies. *Biochemistry*. **52** (24), 4107-4126, (2013).
23. Sui, D., Liu, M., & Kuo, M. H. In vitro aggregation assays using hyperphosphorylated tau protein. *Journal of Visualized Experiments*. (95), e51537, (2015).
24. Apetri, A. *et al.* A common antigenic motif recognized by naturally occurring human VH5-51/VL4-1 anti-tau antibodies with distinct functionalities. *Acta Neuropathologica Communications*. **6** (1), 43, (2018).

25. Barghorn, S., Biernat, J., & Mandelkow, E. Purification of recombinant tau protein and preparation of Alzheimer-paired helical filaments *in vitro*. *Methods Mol Biol.* **299** 35-51, (2005).
26. Zhu, H. L. *et al.* Quantitative characterization of heparin binding to Tau protein: implication for inducer-mediated Tau filament formation. *Journal of Biological Chemistry.* **285** (6), 3592-3599, (2010).
27. Buee, L., & Delacourte, A. Comparative biochemistry of tau in progressive supranuclear palsy, corticobasal degeneration, FTDP-17 and Pick's disease. *Brain Pathology.* **9** (4), 681-693, (1999).